Dehydroacetic acid Derived Schiff base as Selective and Sensitive Colorimetric Chemosensor for the Detection of Cu(II) ions in Aqueous Medium

Devika Vashisht[a], Shikha Sharma[a], Rakesh Kumar[a], Vaneet Saini[a], Vikram Saini[b], Alex Ibhadon[c], Subash Chandra Sahoo[a], Shweta Sharma[d], S. K. Mehta[a]* and Ramesh Kataria[a]*

[a] Department of Chemistry and Centre of Advanced Studies in Chemistry Panjab University, Chandigarh 160014, India
[b] Department of Biotechnology, All India Institute of Medical Sciences (AIIMS), New Delhi, Delhi-110029, India
[c] Department of Chemical Engineering, University of Hull, Hull HU6 7RX, United Kingdom
[d] Institute of Forensic Science and Criminology, Panjab University, Chandigarh 160014, India

Corresponding Email: skmehta@pu.ac.in, rkataria@pu.ac.in

Abstract

The deficiency, as well as overconsumption of essential metal ions, has serious health implications. Hence, the design and synthesis of sensors for accurate detection of such ionic species are of great significance. We report the synthesis and characterization of a yellow-coloured Dehydroacetic acid-based chemosensor DHB ((E)-N-(1-(2-hydroxy-6-methyl-4-oxo-4H-pyran-3-yl) ethylidene) benzohydrazide for a quick and affordable copper detection. A naked-eye visible colour transition from light yellowish to bluish green was observed instantly following Cu^{2+} addition. DHB did not yield colour change with any other ionic species indicating its specificity. The binding of DHB to Cu^{2+} caused a blue shift accompanied by an increased intensity due to an intramolecular charge transfer (ICT). No interference from competitive ionic species reiterated the selectivity of this probe. The outcomes of single-crystal X-ray analysis, titration studies, and Job's plot indicated a 1:2 stoichiometry between Cu^{2+} and DHB. The experimental results matched well with the theoretical results obtained from Density Functional Theory (DFT) calculations. The practical applicability of the probe for Cu^{2+} estimation was further determined using water samples from various sources. The sensor could detect copper as low as 0.156 μM in an aqueous media which is very less than the permissible value of 20 μM in water.

Keywords

Colorimetric detection; Cu(II); Schiff’s base; Chemosensor; Dehydroacetic Acid

1. Introduction

The sensing technology has evolved significantly to develop well-equipped molecular sensors to monitor biologically and environmentally important metal ions [1]. Metals are natural ingredients of the Earth’s crust. Natural and man-made activities cause their discharge into the environment. These metal ions enter the complex biological systems following different pathways like food, air, drinking water, etc. and subsequently lead to bioaccumulation over a period of time [2]. Although metal ions are crucial for the growth and development of complex biological systems [3], however, their over-consumption may cause serious side-effects and hence metal levels in food/water needs to be monitored.

The fabrication and implementation of colorimetric chemosensors for the detection of such ionic species is a better option than the sophisticated and complicated conventional instrumentations [4,5]. The conventional instrumentation techniques available for detection of the metallic species involve time-consuming pre-sample treatment, complex experimentation and sophisticated handling, which limits their routine application. In contrast, chemosensors have come out as superior alternatives due to their cost-effectiveness, and easy operation [6,7].

A chemosensor is a chemical system which has the ability to bind with a specific target analyte causing an alteration in one or more assets of the system in the form of colour, fluorescence or redox potentials [8]. The advances in the synthesis of chemosensors for tagging biologically and environmentally essential ions has received spotlight because of their significant roles in industry, living systems, photo-sensitization, drug development, environmental monitoring, cancer detection and human health [9,10]. Among different chemosensors, colorimetric chemosensors are easy to apply as they allow detection of a specific target by inducing a colour change and do not require complicated pre-sample preparation [4,8,11-13]. Schiff’s bases form one class of the different colorimetric chemosensors which are used for signaling and monitoring the ionic species in an aqueous medium. They have a capability to bind to a specific target through imine nitrogen and stabilize the target species depending upon the signature size of the cavity and target ionic species. Schiff’s bases are also known for anti-bacterial, anti-tuberculosis, anti-carcinogenic properties, etc. [14]. Several Schiff base entities have been reported and used for the fluorometric and colorimetric detection of metal ions specifically Cu^{2+} [15-19]. Copper (Cu) is the third most common transition element (after Iron and Zinc) in the human body with prescribed consumption limits [20, 21]. US Environmental Protection Agency (EPA) has set 20 µM of copper in drinking water as the upper limit [22-24]. Copper is essential for maintaining healthy metabolism in humans [25]. The deficiency of copper can lead to myeloneuropathy, fatigue, weak and brittle bones, pale skin and while the exceeding exposure to copper can trigger neurodegenerative disorders, renal damage, and oxidative stress. Inadequate levels of copper can cause Wilson's and Alzheimer's disease [15-18, 26].

Yang et *al.* [27], Mergu et *al.* [28] Manhanshi et *al.* [29], Razak et *al.* [30], Mohammadi et *al.* [31] and Manna et *al.* [32] synthesized diphenyl-derived salicylhydrazone Schiff's base, (E)-N′-((7-(diethylamino)-2-oxo-2H-chromen-3-yl)methylene)-3,4,5-trimethoxybenzohydrazide, 1N-allyl-2-(2, 5-dimethoxyphenyl)-4, 5-diphenyl-1H-imidazole, Chromone-based colorimetric sensor, bis-thiourea (BT) ligand compound, N,N′-(((3,3′-dimethoxy-[1,1′-biphenyl]-4,4′-diyl)bis(azanediyl))bis(carbonothioyl))bis(4-methoxybenzamide) based microspheres and N-(2-hydroxybenzylidene)-2-(benzamido) benzohydrazide which were used for the sensing of Cu^{2+}. However, these ligands offer many disadvantages including a higher ratio of organic solvents in the solvent system and limit of detection. The objective of the present work was to synthesize modified Schiff base DHB ((E)-N-(1-(2-hydroxy-6-methyl-4-oxo-4H-pyran-3-yl) ethylidene) benzohyrazide) by setting a condensation reaction between benzohydrazide and DHA. The chemosensor DHB was used for the purpose of sensing Cu^{2+}, to achieve lower detection limit and naked eye visible detection without much use of organic solvent. The proposed chemosensor DHB could detect copper as low as 0.156 μM in an aqueous medium which is very less than the prescribed value of 20 μM set by US EPA.

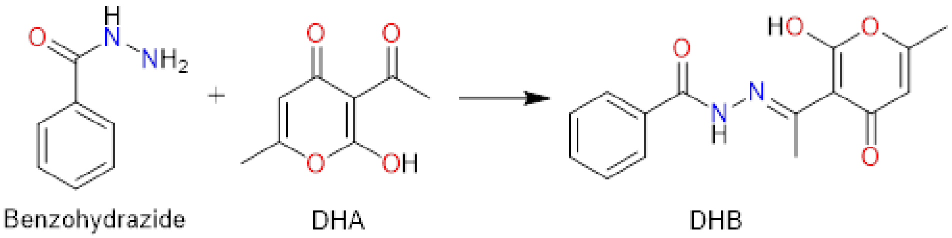

Scheme 1. Synthesis route for the chemosensor DHB

2. Experimental

2.1. Materials

Ethyl benzoate, hydrazine hydrate, and Dehydroacetic acid (DHA) were bought from commercial supplier Sigma Aldrich and were used without further purification. Ethanol was ordered from ChangsuYanguan Chemicals. The solution of all the cations (Ce^{3+}, Pb^{2+}, Hg^{+}, Cd^{2+}, Ag^{+}, Pd^{2+}, Zn^{2+}, Cu^{2+}, Ni^{2+}, Co^{2+}, Mn^{2+}, Fe^{2+}, Cr^{3+}, Ca^{2+}, K^{+}, Na^{+}) were made by dissolving their nitrates and acetates in double-distilled water. Metallic salts were purchased from Alfa-Aesar. The buffer solutions were made using 4-(2-hydroxyethyl)-1-piperazineethanesulfonic acid (HEPES) procured from Avra Synthesis. pH studies were performed by using an appropriate amount of sodium hydroxide and hydrochloric acid. All the glassware was washed using aqua regia.

2.2. Instrumentation

Fourier Transform Infrared (FT-IR) spectra were logged on Thermo Scientific Nicolet iS-50 spectrometer in the range 4000-400 cm^{-1}. A 10 mm path length quartz cuvette was used to record UV-vis spectra in the wavelength range 200-800 nm on a Perkin Elmer Lambda 750 UV/Vis/NIR spectrophotometer. ^{1}H-NMR of the synthesized probe DHB in deuterated Trichloromethane ($CDCl_3$) as a solvent was recorded on Bruker DRX spectrometer using (TMS) trimethylsilane as an internal reference. The pH values were noted down using calibrated Cole Parmer P200 bench-top digital pH meter.

2.3. Method

The colorimetric chemosensor (Scheme1) DHB ((E)-N-(1-(2-hydroxy-6-methyl-4-oxo-4H-pyran-3-yl) ethylidene) benzohyrazide) was synthesized according to the reported method [30] by setting a one-pot condensation reaction between benzohydrazide and DHA. For the synthesis of benzohydrazide, hydrazine hydrate was added to the ethanolic solution of ethyl benzoate followed by refluxing at 60 °C. The precipitates were obtained after 7 h of reflux. The white compound was carefully filtered, washed several times with ethanol and finally dried in a vacuum desiccator. For the synthesis of DHB, DHA was added to an ethanolic solution of benzohydrazide and the solution was stirred for 24 h at room temperature. The yellow product was obtained, filtered and dried in a vacuum desiccator. The DHB is completely solvable in solvents like methanol, ethanol, chloroform, dimethyl sulphoxide (DMSO) and dimethyl formamide (DMF).

2.4. Crystallography studies

Crystal of Cu(II)-DHB was mounted on Hampton Cryo-loop. The geometric and intensities data for the crystals was collected using a Super-Nova (Mo) X-ray diffractometer equipped with a micro-focus sealed X-ray tube Mo-Kα ($\lambda = 0.71073$ Å) X-ray source and HyPix3000 (CCD plate) detector of with increasing ω (width of 0.3 per frame) at a scan speed of either 5 or 10 s/frame. All the data were collected at room temperature. Data acquisition and extraction were done using the CrysAlisPro software. Using Olex2 [34], the structure was solved with the SIR2004 [35] structure solution program using Direct Methods and refined with the ShelXL [36] refinement package using Least Squares minimization. All non-hydrogen atoms were refined with anisotropic thermal parameters.

2.5. Selective Cation Recognition Studies

DHB was found to be soluble in a solvent system comprised of 80 parts of distilled water and 20 parts of ethanol. The metal ion sensibility was checked by additional dilution of 1 mM stock solution of DHB prepared in solvent system viz 80:20 distilled water: ethanol. The cation recognition experiment was conducted by addition of 0.75 μM of each metal salt solution to 10 μM of detector DHB. The difference in the spectral behaviour was observed using UV-vis spectroscopy. All the solutions prepared were left as such for nearly 15 minutes to allow complete complexation of DHB with cationic species.

2.6. pH Studies

To evaluate the effect of pH on sensing capability of DHB, a range of solutions with pH 2-11 was prepared by using HEPES buffer. An appropriate amount of sodium hydroxide/hydrochloric acid was added to regulate the pH. A 1 mM stock solution of DHB was prepared by dissolving it in 80:20 distilled water: ethanol. A 0.1 ml aliquot from the stock solution of DHB was added to 5 μM of Cu^{2+} prepared in HEPES buffer and scanned using UV-vis spectroscopy. HEPES buffer was selected because of its negligible binding ability with metal ions. Also, the HEPES buffer does not absorb in UV-vis range which makes it suitable for the proposed system [37-39].

2.7. Titration Studies

Although the probe could sense the Cu^{2+} at the original pH, the best performance was found at pH = 6 which is quite close to neutral pH. The titration studies were done at optimized pH = 6 and the absorption trend with a change in concentration was observed. A range of solutions with

Cu^{2+} concentration from 0.24 to 3.5 μM in HEPES buffer using 10 μM of DHB were made and scanned using UV-vis spectroscopy.

2.8. Real samples of water

For the real-time applicability of the chemosensor, various samples like distilled water, drinking water, sea-water, and river water were collected and spiked with a known concentration of Cu^{2+}. Sea water was taken from the Arabian Sea (Mumbai, India) and River water from the Saraswati River (Haryana, India). All the real water samples were filtered to remove solid impurities using Whatman filter paper. The drinking water sample was collected from the domestic water supply.

2.9. Computational Studies

The input files of Cu(II)-DHB complex and DHB were organized using GaussView 6.0.16. All the computational calculations were performed on Gaussian 09 rev. D.01 using DFT method. The optimized minimum energy structures were obtained by using exchange-correlation functional B3LYP/GEN and 6-31G (d,p) basis set for N, O, C, H atoms and LANL2DZ basis set for Copper atom in the gas phase. GEN keyword combined 6-31G (d,p) and LANL2DZ basis sets. Evident from the analysis of vibrational frequencies, the optimized structures of organic moieties were found to be stationary points corresponding to local minima without imaginary frequencies.

3. Results and Discussion

The UV-vis absorption plot (Figure 1) of yellow-coloured product DHB exhibited an absorption band around 260 nm attributed to the $\pi \rightarrow \pi^*$ transitions of the aromatic ring. The $n \rightarrow \pi^*$ transitions of less energy from the lone pair of N in C=N bond to the π bond of the aromatic ring were accountable for the band centred at 360 nm. The FT-IR spectrum of the receptor DHB revealed a peak at 1643 cm^{-1} ascribed to imine C=NH of the receptor. The sharp peak located at 8.45 ppm of the ^{1}H-NMR spectra of the DHB signified the successful creation of azomethnic C=NH bond in the receptor (Figure S1).

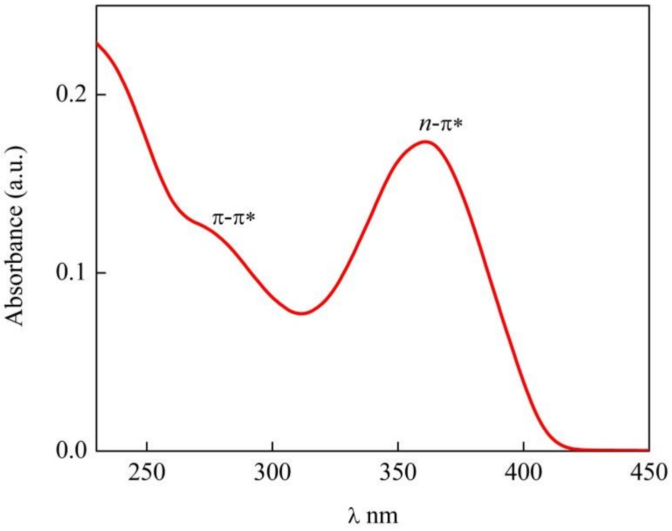

Figure 1. UV-vis spectrum of the synthesized probe DHB

Table 1. Spectroscopic data for DHB

Compound	IR stretching (cm^{-1})	UV-vis absorption peak (nm)	^{1}H-NMR (ppm)
DHB	1643 ($\nu_{C=N}$) 1656 ($\nu_{C=O}$)	λ_{abs} = 260 ($\pi \rightarrow \pi$ *) λ_{abs} = 360 ($n \rightarrow \pi$ *)	7.1-8 (aromatic H) 8.5 (C=NH)

3.1. Cation selectivity studies

The performance of the receptor DHB was probed after addition of various cationic species such as Ag^+, Hg^{2+}, Ni^{2+}, Ba^{2+}, Pb^{2+}, Na^+, Mn^{2+}, Mg^{2+}, Al^{3+}, Ca^{2+}, K^+, Fe^{2+}, Zn^{2+}, Cr^{3+}, Co^{2+}, Ce^{3+}, Cd^{2+}, Cu^{2+}, and Fe^{3+}(Figure 2). Modification of optical behaviour in terms of drastic change in the colour of DHB on the addition of Cu^{2+} from colourless to bluish green colour was observed which gave the confirmation of its complexation (Figure 3). A blue shift in the UV-vis absorption spectrum of DHB upon addition of Cu^{2+} substantiated the complexation with the DHB.

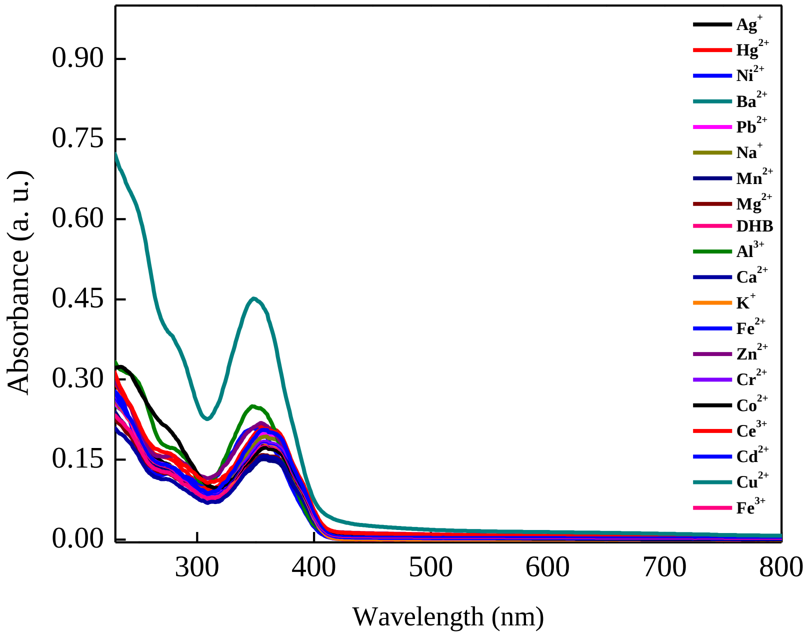

Figure 2. Absorption spectral changes of DHB (10 μM) after the addition of equimolar concentrations of various cations

No noteworthy change was seen after the addition of an equimolar solution of other cationic species. The instant colour change of the solution containing DHB following the addition of Cu^{2+} highlighted its suitability for real-time analysis.

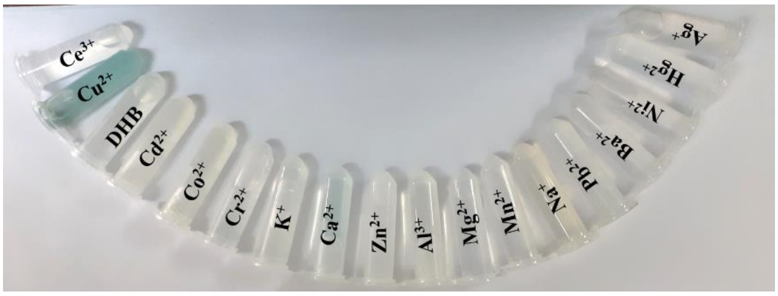

Figure 3. Naked eye visible colour changes induced in DHB (ethanol: water in 8:2 v/v) after equimolar addition of different metal ions (20 μM)

3.2. FT-IR investigation

The FT-IR spectrum of the fabricated probe DHB (Figure 4) exhibited a strong azomethinic vibration around 1643 cm^{-1}. After complexation with Cu^{2+}, the azomethinic stretching vibration

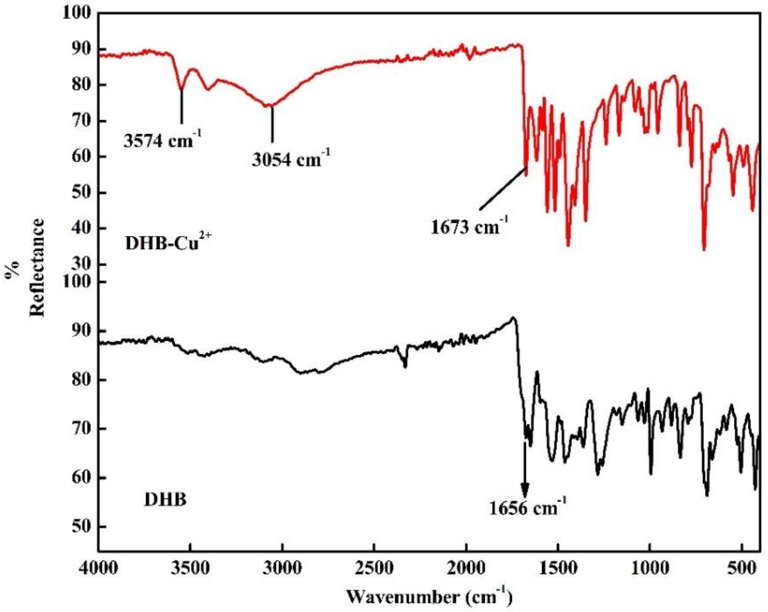

Figure 4. FT-IR spectrum of DHB and its Cu^{2+} complex

shifted to 1617 cm^{-1}. The vibrations due to lactonic C=O of the group of DHB drifted from 1656 cm^{-1} to 1673 cm^{-1} in Cu(II)-DHB [40]. The N-H stretching vibrations were visible at 3104 cm^{-1}. The signals around 1437 & 677 cm^{-1} were due to O-H in-plane and out plane bending of DHB, respectively. The aliphatic signal vibrations were observed at 2893 and 3390 cm^{-1}. The spectrum exhibited $\nu_{C\text{-}O}$ stretching in 1130-1300 cm^{-1} range which is due to phenolic C-O stretching. In Cu(II)-DHB, Cu-O and Cu-N stretching signals appeared at 535 cm^{-1} and 660 cm^{-1}, respectively [41]. The signal in the range 3200-3400 cm^{-1} broadened due to extensive hydrogen bonding. The C=N stretch shifted to 1617 cm^{-1} after complexation with Cu^{2+}. A drastic variation in the C=O and C=N stretch suggested coordination through C=O and C=N.

3.3. Crystal Structure

Addition of DHB to the solution of Cu^{2+} transformed the solution from colourless to green. The observed change was due to the formation of Cu(II)-DHB complex between the receptor and the target ion in ethanol and water (2:8) mixture. The complex Cu(II)-DHB crystalized in the triclinic system with *P*-1 space group. The asymmetric unit contained one Cu-metal centre and two ligands and a coordinated water molecule. The Cu-center adopted a distorted square pyramidal geometry where one of the ligands coordinated to the metal in a tridentated fashion via ONO coordination pocket (Figure 5). The crystallographic parameters are shown in table S1. The fourth position was engaged with a water molecule in the equatorial plane while the apical fifth position was occupied by the O-atom of the DHB moiety of another ligand with a bond distance of 3.621 Å which is common for the Cu-square pyramidal system. The equatorial Cu−O bond lengths were within the range of 1.8821(15) -1.9813(16) and that of Cu-N of 1.9144(18) Å.

The water molecule positioned in equatorial place, H-bonded via both inter and intra-molecular mode with a distance of 2.776 and 2.788 Å with O-atoms of amide and DHA molecule respectively. The protonated -NH-NH group was H-bonded with O-atoms of DHA moiety of the coordinated ligand.

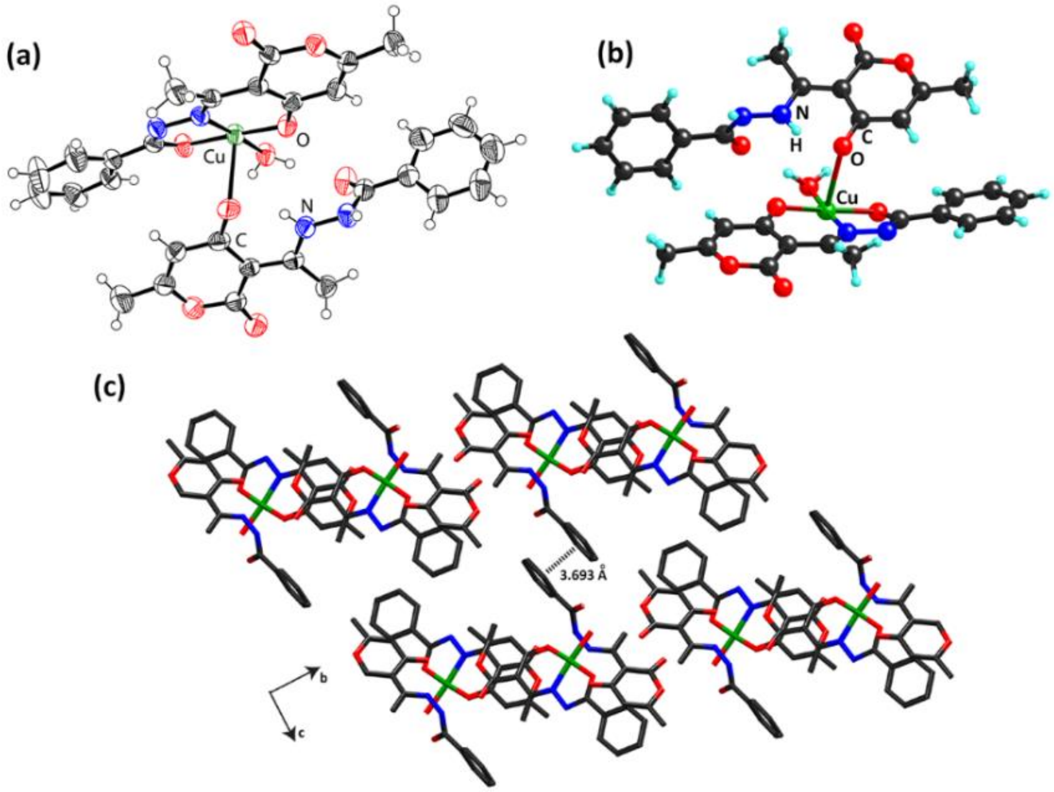

Figure 5. (a) Ortep diagram of Cu(II)-DHB with 30% thermal ellipsoid; (b) Optimized structure of Cu(II)-DHB; (c) Lattice picture of the molecule along ac-plane showing a 1D chain of molecules formed due to various H-bonds

A 1D chain of molecules thus formed due to various H-bonds along *ac*-plane and the list is given in the table S2. In the *bc*-plane, clear π-π interaction formed between the aromatic groups of two adjacent the complexes with a distance of 3.693 Å (Figure 5c) was observed, resulting in a layer like an arrangement. Both the N-atoms of the partially coordinated ligand were protonated leaving the hydroxide O-atom to coordinate with metal. The

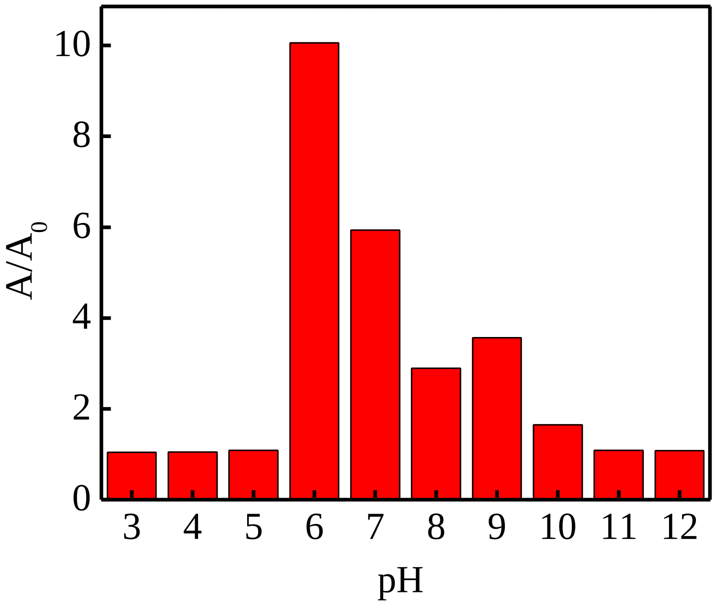

Figure 6. Absorbance alteration of DHB under different pH conditions after the addition of Cu^{2+}

charge neutrality and fully coordinated ligand were responsible for charge balancing of the Cu-center.

3.4. Effect of pH

The UV-vis scans were logged for DHB before and after the addition of Cu^{2+}. Figure 6 illustrates the results of the pH studies conducted for the sensor. It is evident that the probe exhibited excellent performance in the pH range 6-7, which is also physiologically relevant. The sensing behaviour of the probe enhanced as the pH of the system increased towards the neutral conditions. The protonation of N of the azomethnic linkage at extreme acidic conditions and the formation of hydroxides at extreme basic conditions were responsible for the lower sensitivity of DHB at extreme pH i.e. 3-5 or 10-12. This broad range ensures a supreme performance of the sensor in close to the neutral condition, thereby making it applicable to a wide range of aqueous samples.

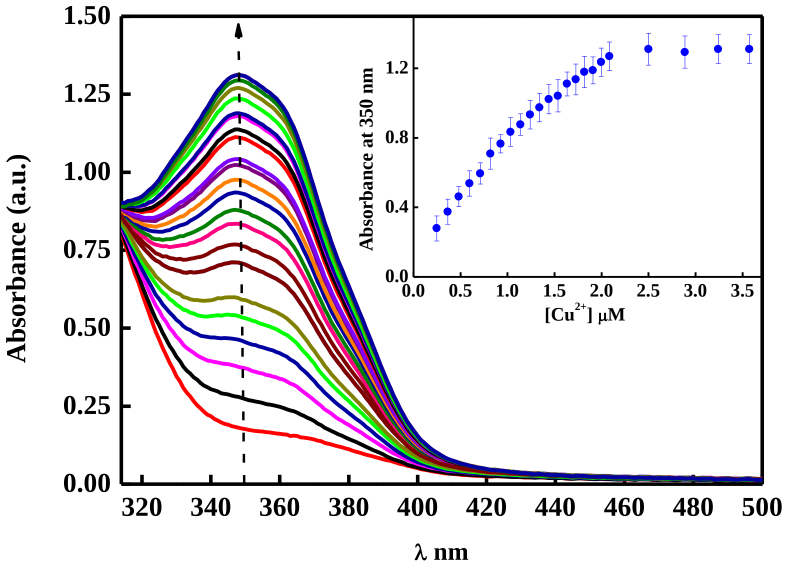

Figure 7. UV-vis absorption spectral changes of DHB (10 μM) after addition of different Cu^{2+} concentrations. Inset: Absorbance at 350 nm v/s Cu^{2+} concentrations

3.5. Titration Studies

After the analysis of the effect of pH on the sensing procedure, the absorption changes of DHB with increasing Cu^{2+} concentration were observed (figure 7). A well-defined blue shift (Δλ~15nm) was observed on successive addition of the analyte i.e. Cu^{2+}. The selectivity of DHB particularly for Cu^{2+} can be

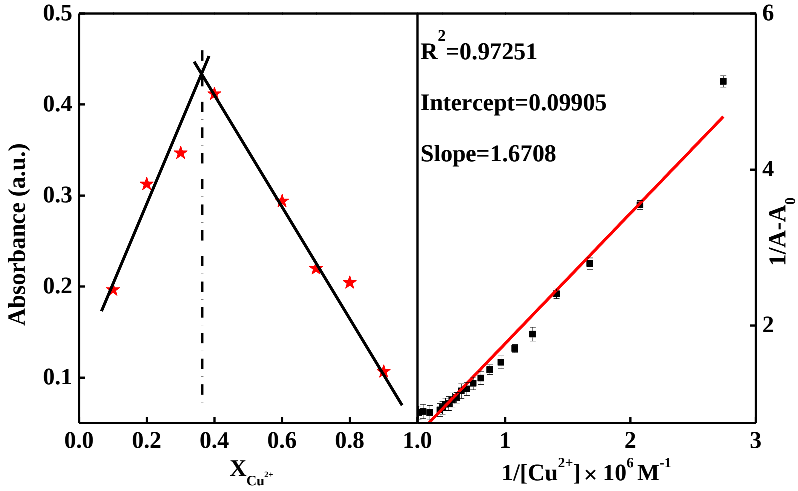

Figure 8 (a) Job's plot for the stoichiometric ratio of the complexation product between DHB and Cu^{2+} under invariant total concentration of DHB and Cu^{2+} (b) Benesi-Hildebrand plot for the estimation of binding constant

attributed to ICT. The excitation by light causes ICT from an electron donor (heteroatoms) to electron acceptor (aromatic ring). The binding of Cu^{2+} to nitrogen and oxygen in conjugation with aromatic ring originated the blue shift in UV-vis spectra [42]. Nonetheless, the contribution of the paramagnetic effects of Cu^{2+} to these optical changes is also a possibility and cannot be ruled out. Likewise, the d-d and f-f transitions are weakly allowed because of the Laporte rules. Another evidence of the complexation was the HRMS spectrum (Figure S7) of the Cu^{2+} complex of DHB which clearly showed a peak at m/z = 634.09.

As evident from the single-crystal X-ray analysis, a 1:2 binding stoichiometry was observed between Cu^{2+} and DHB (Figure 5). The plot of the absorbance versus the concentration of Cu^{2+}displayed a linear region from 0.24 μM to 2.00 μM. The limit of detection (LOD) as calculated by 3σ criterion [43] came out to be 0.156 μM. To further investigate the binding constant and validate the stoichiometry of binding between DHB and Cu^{2+}, the results of the Benesi-Hildebrand [44] and Job's plot [45,46] were examined. The association constant and binding ratio were evaluated using the Benesi-Hildebrand equation (1)

$$\frac{1}{A-A_0} = \frac{1}{K(A_{max}-A_0)[Cu^{2+}]^1} + \frac{1}{A_{max}-A_0} \qquad (1)$$

`The linearity of the Benesi-Hildebrand plot indicated the presence of one metal centre in the complex (Figure 8b). The Job's plot of the absorptions of the varied mole fraction of Cu^{2+} by keeping the total concentration of DHB & Cu^{2+}invariant was analyzed. As expected, the maximum at a 0.33-mole fraction of the Job's plot (Figure 8a) further validated 1:2 stoichiometric ratio of the complex formed between Cu^{2+} and DHB. The comparison of the solvent system, selectivity, detection limit, and fabrication process was made with the previously reported sensors (Table S3). The previously reported probes display shortcomings in comparison to the proposed probe in terms of the solvent system and detection limit.

3.6. Interference Studies

To investigate the selectivity of the probe DHB towards Cu^{2+}, competitive studies were done with other metal ions Ag^{+}, Al^{3+}, Ba^{2+}, Ca^{2+}, Cd^{2+}, Ce^{3+}, Co^{2+}, Cr^{2+}, Fe^{2+}, K^{+}, Mg^{2+}, Na^{+}, Ni^{2+}, Pb^{2+}, Zn^{2+}, Hg^{2+}, $Mn^{2+}$and Fe^{3+} in the presence of Cu^{2+} (10 μM). To carry out the competitive experiments, a number of DHB solutions containing equimolar metal ion species after addition of Cu^{2+}were scanned for absorption. The competitive studies were conducted for 50 μM (Figure 9), 100 μM and 150 μM of competitive ions (Figure S2). As clear from figure 9, no significant interference was observed for any cationic species [40,47,48]. This capability of the probe DHB to exclusively sense the Cu^{2+} even with the simultaneous presence of other metal ions entitles its suitability as a useful copper sensor.

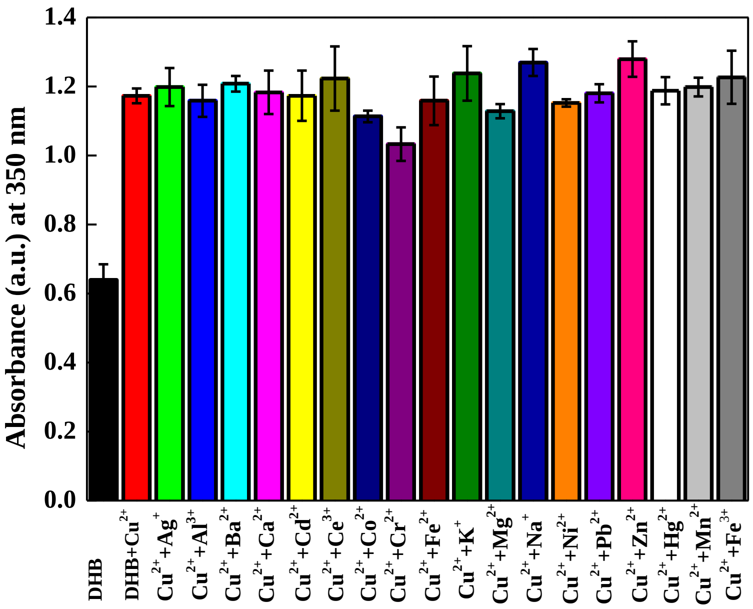

Figure 9. Interference studies for the selectivity of the chemosensor DHB towards Cu^{2+} (10 μM) in the co-existence of other cationic species (50 μM)

3.7. Application on real samples

To investigate the real-time applicability of the chemosensor DHB, samples collected from different water sources were analyzed. Each of the water sample collected was spiked with a known amount of Cu^{2+} and was analyzed for its tendency to sense Cu^{2+}. The amount of Cu^{2+} in each of the sample was calculated using the calibration curve (Figure 7). Figure 10 shows the visible colour transitions observed in all the water samples and confirmed the ability of the sensor to sense Cu^{2+}. The recoveries and LOD values obtained for each of the water samples (Figure S3) are listed in Table 2.

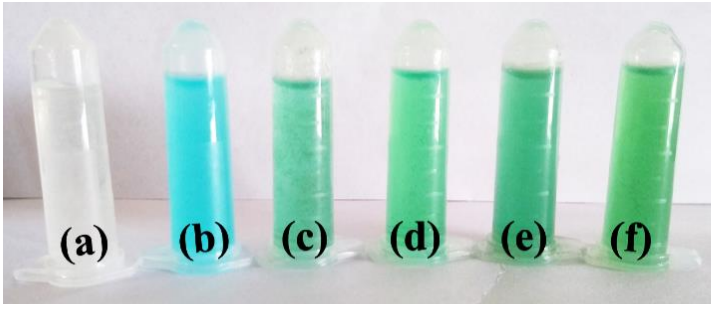

Figure 10. Colour of (a) DHB only (b) Cu^{2+} only and change in colour of DHB after addition of Cu^{2+} solution (c) in sea water (d) distilled water (e) river water and (f) drinking water

Table 2. Estimation of Cu^{2+} in different water samples collected from various sources

Sample	**Added (μM)**	**Found (μM)**	**Recovery % (mean ± S.D)**	**LOD (μM)**
Sea Water	0.25	0.247	98.8 ± 0.10	0.589
	1.53	1.538	100.5 ± 0.05	

	2.50	2.494	99.76 ± 0.11	
Drinking Water	0.25	0.256	102.4± 0.10	0.580
	1.53	1.546	101.0± 0.08	
	2.50	2.482	99.28± 0.05	
River Water	0.25	0.246	98.4± 0.09	0.513
	1.53	1.539	100.5± 0.04	
	2.50	2.52	100.8± 0.10	
Distilled Water	0.25	0.258	103.2± 0.10	0.492
	1.53	1.535	100.3± 0.05	
	2.50	2.479	99.1± 0.10	

3.8. Response time and Stability

To determine the efficacy of the probe for real-time analysis, the response time of the DHB to tag the target and stability of both DHB and the complex formed after the interaction of the analyte with probe plays a fundamental role. The response time is the time interval after which a saturated absorbance plot is achieved in the presence of a fixed amount of Cu^{2+}. Application of the DHB to the samples prompted an instant colour change to green following Cu^{2+} addition. Since it took ~3 minutes to scan and record the UV-vis spectrum, the response time can be stated to be less than 3 min. Figure S4 displays the plot of absorbance at 350 nm versus time. The stability of DHB and the Cu(II)-DHB complex was evaluated by recording the absorbance for a significant time period. The absorption spectra of the DHB and Cu(II)-DHB for 3.5 h at the interval of 15 min were logged. The UV-vis spectrum was recorded after 6 months also. The absence of any significant change in UV-vis absorbance specified the stability of both the DHB (Figure S5) and Cu(II)-DHB complex further substantiating the field application of this sensor towards copper detection (Figure S6).

3.9. DFT Study

The geometry optimization for Cu(II)-DHB complex was done at the mixed level of theory using Gaussian 09 [49] with 6-31G (d,p) and LANL2DZ, whereas for the free ligand (DHB) 6-31G (d,p) basis set was employed (Figure 11). The absence of imaginary frequency for the optimized structures designated the local minima of their geometries.

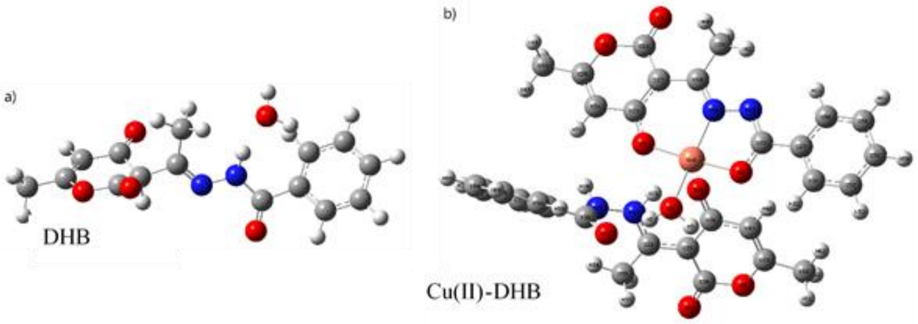

Figure 11. DFT optimized geometry of the a) DHB ligand b) Cu(II)-DHB complex

Atomic charge distribution between donor sites and acceptor sites were estimated by natural population analysis (NPA) in the gas phase. By comparing the atomic charges, it was observed that the electron density on Cu(II) cation increased after complexation. For instance, before complexation, the formal charge on Cu(II) was +2, whereas the charge on Cu in (Cu(II)-DHB) is + 0.934. This clearly indicated transfer of negative charges from the donor atoms of the DHB to the Cu(II) ion during complex formation.

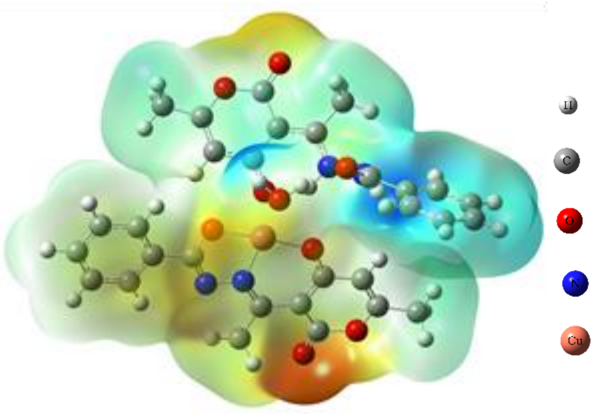

Figure 12. Molecular electrostatic potential surface of Cu(II)-DHB complex. The electrophilic regions are represented by red, nucleophilic by blue and neutral electrostatic potential by green

Molecular Electrostatic Potential (MEP) is an important tool to analyze the electrophilic and nucleophilic sites which facilitate recognition of hydrogen-bonding interactions and physical properties like electronegativity, chemical reactivity and dipole moment. The MEP surface was mapped on the optimized geometry of the complex (Figure 12). The electrophilic regions were observed to be mainly concentrated on the carbonyl group of the amide (represented by red color). On the other hand, the conjugated carbonyl group and hydrogens of the aromatic ring represented sites of positive electron density. The energy gap of highest occupied molecular orbital (HOMO) and lowest unoccupied molecular orbital (LUMO) reflect several characteristic attributes of a molecule [50-52]. For instance, a molecule having a small frontier orbital gap is associated with high polarizability and generally exhibit high chemical reactivity and low kinetic stability. The energies associated with HOMO and LUMO for Cu(II)-DHB complex were calculated using the B3LYP method and 6-31G (d,p)/LANL2DZ basis sets in the gas phase. The HOMO of α-and β-orbitals were observed to be mainly concentrated around amide of the DHB ligand directly bonded to the Cu^{2+}. The LUMO of α-orbitals concentrated on the hydrazone functionality of the bonded DHB ligand, whereas LUMO of β-orbitals was on the conjugated carbonyl group of the free DHB ligand. 3D plots for frontier molecular orbitals (FMO) along with the gap associated with them are illustrated in figure 13. Since HOMO represents an outer

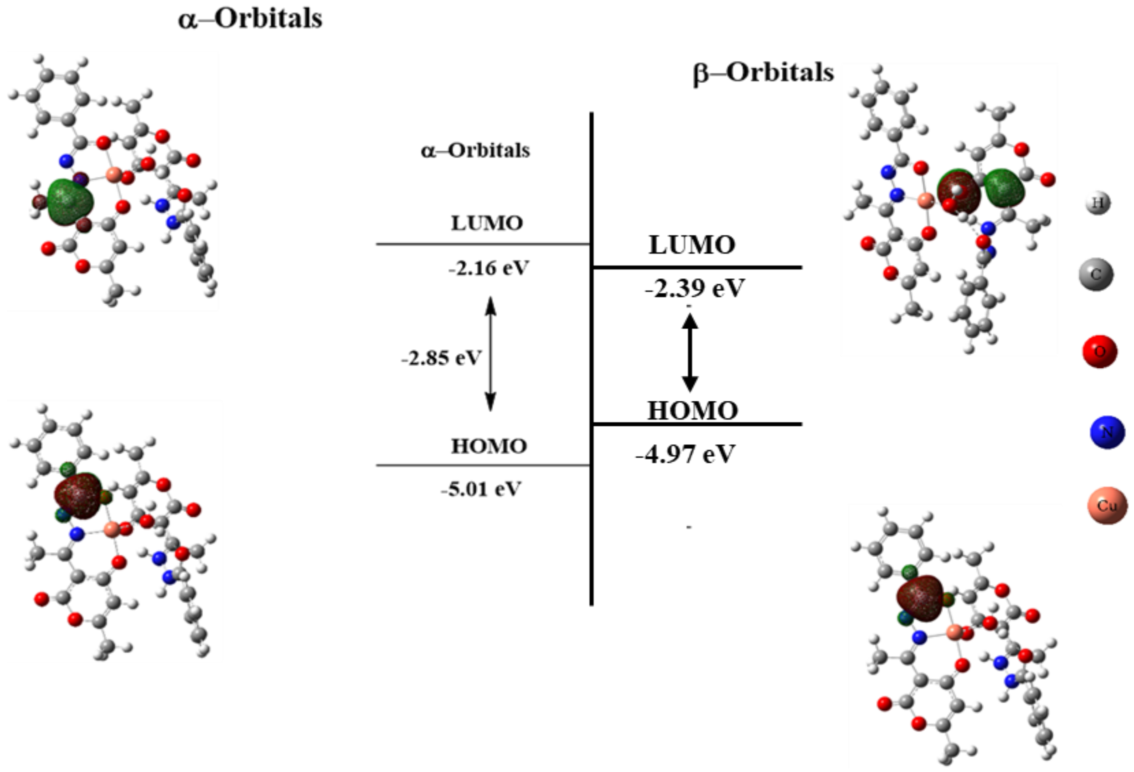

Figure 13. HOMO-LUMO orbital surfaces and energy gap for Cu(II)-DHB complex. Red indicates occupied orbital and green indicates unoccupied orbitals

orbital containing electrons, it acts as an electron donor and hence ionization potential (I) is directly related to the energy of the HOMO. Similarly, LUMO can act as an electron acceptor, therefore, the LUMO energy is directly related to an electron affinity (A). Therefore, both **I** and **A** of Cu(II)-DHB complex were calculated by means of Koopmans theorem with E_{HOMO} and E_{LUMO} values as **I** = $-E_{HOMO}$ and **A** = $-E_{LUMO}$. A measure of the confrontation to change in electron distribution of a moiety can be quantified using chemical hardness (η) of a molecule which in turn is related to the stability and reactivity of a system [53]. The more the value of chemical hardness, lesser is the chemical reactivity and hence greater chemical stability. The stability and reactivity associated with a molecular system can also be characterized using well-known global reactivity descriptors such as electronic chemical potential (μ), global electrophilicity index (ω) and softness (S). All these values are calculated as shown in table 3.

Table 3. Electrostatic results for Cu(II)-DHB complex

Compound	**HOMO (eV)**	**LUMO (eV)**	Chemical hardness $\eta = 1/2\ (I-A)$	Chemical potential $\mu = -1/2\ (I+A)$	Chemical softness $S = 1/2\eta$	Electronegativity $\chi = -\mu$	Electrophilicity index $\omega=\mu^2/2\eta$
Cu-DHB	-4.99	-2.28	1.36	-3.64	0.68	3.64	4.87

Hirshfeld Surface Analysis

The mapping of the Hirshfeld surface in a crystal molecule demonstrates three-dimensional electron density, which gives insight into the strong intermolecular interactions surrounding the molecule in a qualitative and quantitative manner. The Hirshfeld surface analysis was performed by Crystal Explorer3.1as shown in Figure 14 [54].

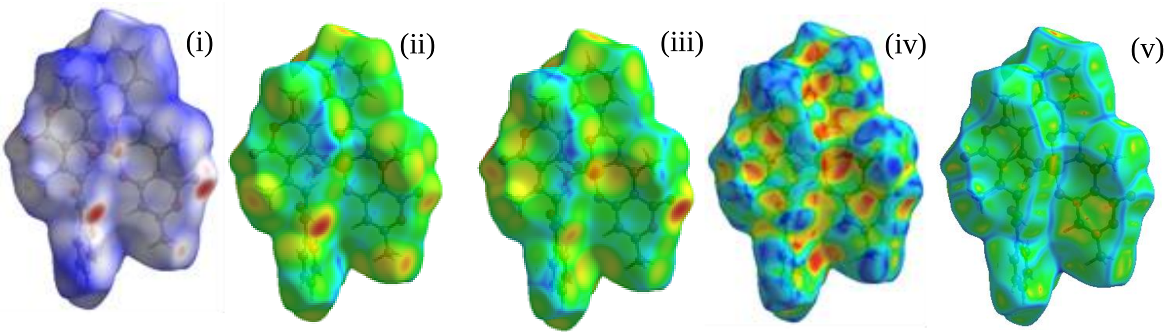

Figure 14. Hirshfeld surfaces mapped over (i) d_{norm}; (ii) d_i; (iii) d_e; (iv) shape index and (v) curvedness for Cu(II)-DHB complex

In the surface analysis, d_e represents the distance of internal atoms to the nearest surface points. However, d_i represents the distance of exterior atoms to the nearest points on the surface [55].

The Hirshfeld surfaces of the Cu(II)-DHB complex were mapped over d_{norm}, d_i and d_e in a transparent manner so that the molecular structure can be visualized around which these properties were calculated (Figure 14).

The appearance of large circular deep-red spots visible on the surface mapped over d_{norm} indicated close contacts particularly hydrogen bonds, however diminutive spots on the surface designated contacts other than hydrogen bonding which are generally weaker and longer (Figure 15 A, B).

The 2D fingerprint plots for the Cu(II)-DHB complex were also mapped for the quantification of intermolecular interactions which were further disintegrated to explore per atom interactions present within the structure are shown in figure 15. A noteworthy molecular interaction of O-H type was reflected which contributed 22.8% of the total surface area of the complex (Figure 15 C-D). It clearly points out the role of hydrogen bonding in the formation and stability of crystal. Also, C-H type contributed 14% of the Hirshfeld surface which originated mainly due to the electrostatic interactions between carbonyl carbon (-**C**=O) of ester and hydrogen attached to the nitrogen of amide(-CON**H**-) as shown in figure 15 E.

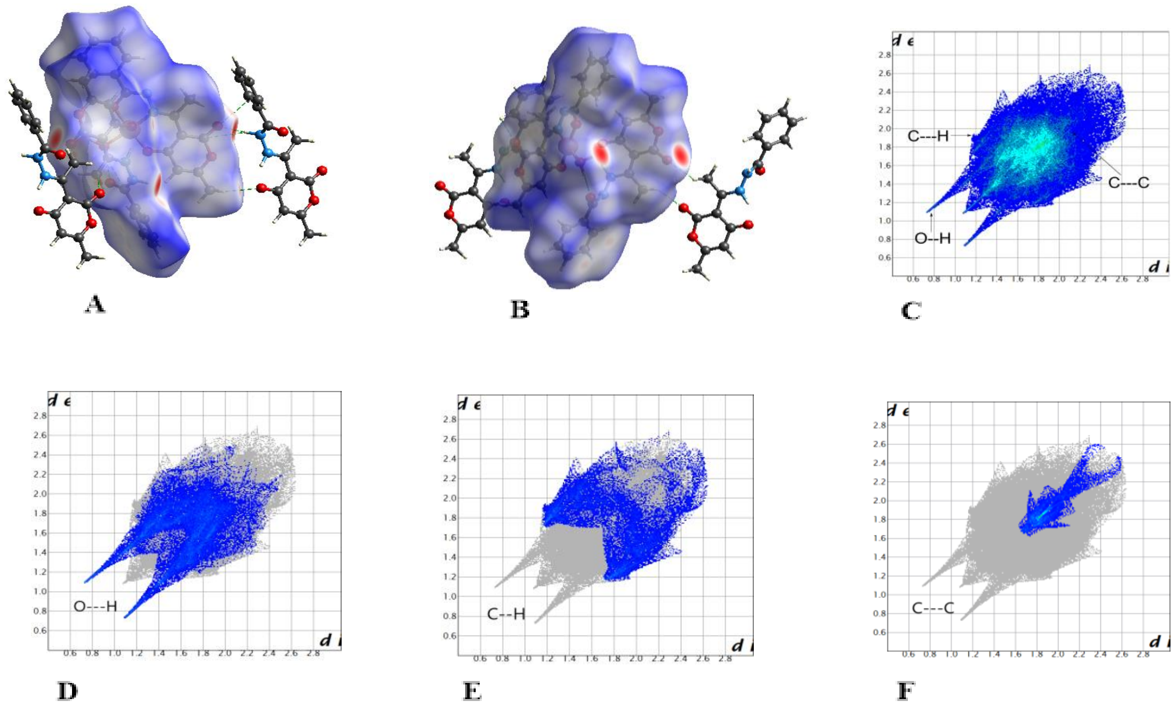

Figure 15. A and B represent views of the d_{norm} Hirshfeld surfaces of Cu(II)-DHB complex in two orientations. C represents close intermolecular contacts between all the atoms. D, E, and F represent close intermolecular contacts between O-H, C-H, and C-C respectively

The calculations revealed that interactions of the C-C type contributed 5.9% mainly arising due to π--π interactions, whereas interactions arising due to N atom were scarce as their contribution came to be only 1.8% of the total intermolecular interactions in the crystal structure figure 15 F.

4. Conclusions

In summary, a selective and sensitive colorimetric chemosensor is synthesized and characterized which can detect the Cu^{2+} in an aqueous medium by producing a visible color change. The proposed chemosensor has many advantages in terms of its solubility in near aqueous medium; its selective, sensitive and instantaneous response for Cu^{2+} in aqueous medium; high efficiency in physiological pH range, its applicability to wide range of field samples of different origins; its LOD value of 0.156 μM and its ability to sense Cu^{2+} even with the co-existence of other ionic species. The cost-effectiveness of the simple synthesis procedure and the excellent performance of the chemosensor makes it appropriate for field investigations and real-time analysis. The overlapping of theoretical and experimental conclusions validated the proposed mechanism. The single-crystal X-ray analysis, Density Functional theory calculations, the Benesi-Hildebrand plot and the Job's plot confirmed the 1:2 stoichiometric binding between Cu^{2+} and DHB. The outstanding performance, easy synthesis, and the synchronized crystal structure results extend its usefulness in the field of optical sensing.

5. Acknowledgements

The authors are thankful to DST, Government of India for PURSE Grant (II) and FIST (II) for Single-crystal facility at the Department of Chemistry, Panjab University, Chandigarh. Vikram Saini acknowledges grant support from Innovative Young Biotechnologist Award (BT/11/IYBA/2018/01) and DST-SERB core grant (CRG/2018/004510). Vaneet Saini recognizes DST for DST-Inspire grant (DST/INSPIRE/04/2017/002529). The authors are also thankful to Sophisticated and Analytical Instrumentation Facility (SAIF)/Central Instrumentation Laboratory (CIL), Panjab University, Chandigarh, India for providing access to necessary instrumentation facilities.

6. References

[1] J. Anastassopoulou, T. Theophanides, The Role of Metal Ions in Biological Systems and Medicine, Bioinorg. Chem. (2013) 209–218.

[2] G. X. Liang, H. Y. Liu, J. R. Zhang, J. J. Zhu, Ultrasensitive Cu^{2+} sensing by near-infrared-emitting CdSeTe alloyed quantum dots, Talanta 80 (2010) 2172–2176.

[3] T. Theophanides, Metal Ions in Biological Systems, Int. J. Quantum Chem. 26 (1984) 933–941.

[4] D. Maity, T. Govindaraju, Highly selective colorimetric chemosensor for Co^{2+}, Inorg. Chem. 50 (2011) 11282–11284.

[5] Z. Liu, X. Jia, P. Bian, Z. Ma, A simple and novel system for colorimetric detection of cobalt ions, Analyst. 139 (2014) 585–588.

[6] K. Kaur, S. Chaudhary, S. Singh, S. K. Mehta, Highly selective probe based on imine linkage for Zn^{2+} and HSO_3^- in mixed aqueous media, J. Lumin. 160 (2015) 282–288.

[7] Y. Wang, L. Wang, L. L. Shi, Z. Bin Shang, Z. Zhang, W. J. Jin, Colorimetric and fluorescence sensing of Cu^{2+} in water using 1,8-dihydroxyanthraquinone-β-cyclodextrin complex with the assistance of ammonia, Talanta. 94 (2012) 172–177.

[8] B. Kaur, N. Kaur, S. Kumar, Colorimetric metal ion sensors – A comprehensive review of the years 2011–2016, Coord. Chem. Rev. 358 (2018) 13–69.

[9] D. Wu, A. C. Sedgwick, T. Gunnlaugsson, E. U. Akkaya, J. Yoon, T. D. James, Fluorescent chemosensors: the past, present and future, Chem. Soc. Rev. 46 (2017) 7105–

7123.

[10] B. Wang, E. V. Anslyn, A Chemosensors Principles, Strategies and Applications, Wiley (2011), ISBN: 978-0-470-59206-9.

[11] X. Tang, J. Han, Y. Wang, L. Ni, X. Bao, L. Wang, W. Zhang, A multifunctional Schiff base as a fluorescence sensor for Fe^{3+} and Zn^{2+} ions, and a colorimetric sensor for Cu^{2+} and applications, Spectrochim. Acta - Part A Mol. Biomol. Spectrosc. 173 (2017) 721–726.

[12] R. Kataria, K. Sethuraman, D. Vashisht, A. Vashisht S. K. Mehta, A. Gupta, Colorimetric detection of mercury ions based on anti-aggregartion of gold nanoparticles using 3,5-dimethyl-1-thiocarboxamidepyrazole, Microchem. J. 148 (2019) 299-305.

[13] R. Kataria, R. Patra, H. K. Sharma, G. Singh, G. Kumar, S. Kumar, Spectrophotometric determination of Tin (II) with 6-Chloro-2-(2'-furyl)-3-Hydroxy-&-Methyl-4-Oxo-4H-1-Benzopyran and its solution state structure study by DFT, Sensor Lett. 15 (2017) 25-31.

[14] A. M. Abu-Dief, I. M. A. Mohamed, A review on versatile applications of transition metal complexes incorporating Schiff bases, Beni-Suef Univ. J. Basic Appl. Sci. 4 (2015) 119–133.

[15] A. K. Manna, K. Rout, S. Chowdhury, G. K. Patra, A dual mode highly selective and sensitive Schiff base Chemosensor for fluorescent colorimetric detection of Cu^{2+}, Photochem. Photobiol. Sci. 18 (2019) 1512.

[16] J. B. Chae, D. Yun, H. Lee, H. Lee, K. Kim, C. Kim, Highly Sensitive Dansyl-Based Chemosensor for Detection of Cu^{2+} in Aqueous Solution and Zebrafish, ACS Omega, 4 (2019) 12537-12543.

[17] D. H. Joo, J. S. Mok, G. H. Bae, S. E. Oh, J. H. Kang, C. Kim, Colorimetric Detection of Cu^{2+} and Fluorescent Detection of PO_4^{3-} and S^{2-} by a Multifunctional Chemosensor, 56 (2017) 8339-8407.

[18] D. Udhayakumari, S. Naha, S. Velmathi, Colorimetric and fluorescent chemosensors for Cu^{2+}. A comprehensive review from the years 2013-2015, Anal. Methods, 9 (2017) 552.

[19] N. Sainin, N. Prigyai, C. Wannasiri, V. Ervithyasuporn, S. Kiatkamjornwong, Green synthesis of fluorescent N, O-chelating hydrazine Schiff base for multi-analyte sensing in Cu^{2+} F^{2} and CN^{-} ions, J. Photochem. Photobiol A. Chem. 358 (2018) 215-225.

[20] H. Y. Kim, H. J. Lee, S. K. Chang, Reaction-based colorimetric signaling of Cu^{2+} ions by oxidative coupling of phenols with 4-aminoantipyrine, Talanta 132 (2015) 625–629.

[21] P. Kaur, D. Sareen, K. Singh, Selective colorimetric sensing of Cu^{2+} using triazolyl monoazo derivative, Talanta 83 (2011) 1695–1700.

[22] N. Wang, Y. Liu, Y. Li, Q. Liu, M. Xie, Fluorescent and colorimetric sensor for Cu^{2+} ion based on formaldehyde modified hyperbranched polyethylenimine capped gold nanoparticles, Sensors Actuators B Chem. 255 (2018) 78–86.

[23] Y. Jiao, L. Zhou, H. He, J. Yin, Q. Gao, J. Wei, C. Duan, X. Peng, A novel rhodamine B-based “off-on’’ fluorescent sensor for selective recognition of copper (II) ions, Talanta. 184 (2018) 143–148.

[24] R. Liu, Z. Chen, S. Wang, C. Qu, L. Chen, Z. Wang, Colorimetric sensing of copper (II) based on catalytic etching of gold nanoparticles, Talanta. 112 (2013) 37–42.

[25] J. Peng, G. Liu, D. Yuan, S. Feng, T. Zhou, A flow-batch manipulated Ag NPs based SPR sensor for colorimetric detection of copper ions (Cu^{2+}) in water samples, Talanta. 167 (2017) 310-316.

[26] S. C. Sahoo, R. Kataria, S. K. Mehta, Copper and its complexes: A pharmaceutical perspective in Chemical Drug Design (Ed. G. K. Gupta, V. Kumar), Berlin, Boston, De Gruyter (2016) 215-236.

[27] Y. Yang, S. Ma, Y. Zhang, J. Ru, X. Liu, H. Guo, A novel biphenyl-derived salicylhydrazone Schiff base fluorescent probes for identification of Cu^{2+} and application in living cells, Spectrochim. Acta Part A Mol. Biomol. Spectrosc. 199 (2018) 202–208.

[28] N. Mergu, M. Kim, Y. Son, A Coumarin-derived Cu^{2+}-fluorescent chemosensor and its direct application in aqueous media, Spectrochim. Acta Part A Mol. Biomol. Spectrosc. 188 (2018) 571-580.

[29] M. N. Mahnashi, A. M. Mahmoud, S. A. Alkahtani, R. Ali, M. M. El-Wekhil, A novel imidazole derived colorimetric and fluorometric chemosensor for bifunctional detection of copper(II) and sulphide ions in environmental water samples, Spectrochim. Acta Part A Mol. Biomol. Spectrosc. 2019 doi.org/10.1016/j.saa.2019.117846.

[30] N. H. A. Razak, L. L. Tan, S. A. Hasbullah, L. Y. Heng, Reflectance chemosensor based on bis-thiourea derivative as ionophore for copper (II) ion detection, 2019, doi.org/10.1016/j.microc.2019.104460.

[31] A. Mohammadi, B. Khalili, A. S. Haghayegh, A novel chromene based colorimetric sensor for highly selective detection of copper ions: synthesis, optical properties and DFT calculations, Spectrochim. Acta Part A Mol. Biomol. Spectrosc. 222 (2019) 571-580.

[32] A. K. Manna, J. Mondal, K. Rout, G. K. Patra, A benzohydrazide based two in one Ni^{2+}/ Cu^{2+} fluorescent colorimetric chemosensor and its applications in real sample analysis and molecular logic gate, Sens. Actuators B Chem. 275 (2018) 350-358.

[33] Rajnikant, Dinesh, Kamni, M. B. Deshmukh, S. D. Desai, B. S. Shinde, P. Kanwal, Synthesis and X-ray structure analysis of benzoic acid [1-(6-methyl-2,4-dioxo-3,4-dihydro-2H-pyran-3-yl)-eth-(E)-ylidene]-hydrazide with a water molecule ($C_{15}H_{14}N_2O_4\cdot H_2O$), J. Chem. Crystallogr. 35 (2005) 357-360.

[34] O. V. Dolomanov, L. J. Bourhis, R. J. Gildea, J. A. K. Howard, H. Puschmann, OLEX2 : a complete structure solution, refinement and analysis program , J. Appl. Crystallogr. 42 (2009) 339-341.

[35] M .C. Burla, R. Caliandro, M. Camalli, B. Carrozzini, G. L. Cascarano, L. De Caro, C. Giacovazzo, G. Polidori, D. Siliqi, R. Spagna, IL MILIONE: A suite of computer programs for crystal structure solution of proteins, J. Appl. Crystallogr. 40 (2007) 609-613.

[36] G. M. Sheldrick, Crystal structure refinement with SHELXL., Acta Crystallogr. Sect. C, Struct. Chem. 71 (2015) 3-8.

[37] D. Vashisht, K. Kaur, R. Jukaria, A. Vashisht, S. Sharma, S. K. Mehta, Colorimetric

chemosensor based on coumarin skeleton for selective naked eye detection of cobalt (II) ion in near aqueous medium, Sensors Actuators B Chem. 280 (2019) 219-226.

[38] U. B. Patel, V. N. Mehta, M. A. Kumar, S. K. Kailasa, 4-Aminothiophenol functionalized gold nanoparticles as colorimetric sensors for the detection of cobalt using UV-Visible spectrometry, Res. Chem. Intermed. 39 (2013) 771–779.

[39] E. J. Song, J. Kang, G. R. You, G. J. Park, Y. Kim, S. J. Kim, C. Kim, R. G. Harrison, A single molecule that acts as a fluorescence sensor for zinc and cadmium and a colorimetric sensor for cobalt, Dalt. Trans. 42 (2013) 15514–15520.

[40] M. S. Hossain, C M Zakaria, Md. K. E. Zaham, B. Zaman, Synthesis, Spectral and Thermal Characterization of Cu(II) Complexes with Two New Schiff Base Ligand towards Potential Biological Application, Der Chem. Sin. 8 (2017) 380-392.

[41] A. K. Gupta, R. Pal, V. Beniwal, Novel Dehydroacetic Acid Based Hydrazone Schiff ’ S Base Metal Complexes of First Transition Series : Synthesis and Biological Evaluation Study, 4 (2015) 990–1008.

[42] Y. J. Zhang, X. P. He, M. Hu, Z. Li, X. X. Shi, G. R. Chen, Highly optically selective and electrochemically active chemosensor for copper (II) based on triazole-linked glucosyl anthraquinone, Dye. Pigment. 88 (2011) 391–395.

[43] S. A. Shahamirifard, M. Ghaedi, S. Hajati, A new silver (I) ions optical sensor based on nanoporous thin films of sol–gel by rose bengal dye, Sensors Actuators B Chem. 259 (2018) 20–29.

[44] O. Garcia-Beltran, N. Mena, L. C. Friedrich, J. C. Netto-Ferreira, V. Vargas, F. H. Quina, M.T. Nunez, B.K. Cassels, Design and synthesis of a new coumarin-based “turn-on” fluorescent probe selective for Cu^{2+}, Tetrahedron Lett. 53 (2012) 5280–5283.

[45] W. Cao, X. J. Zheng, D. C. Fang, L. P. Jin, A highly selective and sensitive Zn (ii) complex-based chemosensor for sequential recognition of Cu (ii) and cyanide, Dalt. Trans. 43 (2014) 7298–7303.

[46] P. F. Hsu, Y. Chen, Synthesis of a Pyrene-Derived Schiff Base and Its Selective Fluorescent Enhancement by Zinc and Aluminum Ions, Int. J. Org. Chem. 08 (2018) 207–228.

[47] S. Y. Kim, S.Y. Lee, J. M. Jung, M. S. Kim, C. Kim, Selective detection of Cu^{2+} and S^{2-} by a colorimetric chemosensor: Experimental and theoretical calculations, Inorganica Chim. Acta. 471 (2018) 709-717.

[48] K. Kaur, S. Chaudhary, S. Singh, S. K. Mehta, Imine modified ZnO nanoparticles: A luminescent chemodosimeter for Al^{3+} and S^{2-} ions based on ligand displacement reaction, New J. Chem. 39 (2015) 1773–1782.

[49] Gaussian 09, Revision D.01, M. J. Frisch, G. W. Trucks, H. B. Schlegel, G. E. Scuseria, M. A. Robb, J. R. Cheeseman, G. Scalmani, V. Barone, B. Mennucci, G. A. Petersson, H.Nakatsuji, M. Caricato, X. Li, H. P. Hratchian, A. F. Izmaylov, J. Bloino, G. Zheng, J. L. Sonnenberg, M. Hada, M. Ehara, K. Toyota, R. Fukuda, J. Hasegawa, M. Ishida, T. Nakajima, Y. Honda, O. Kitao, H. Nakai, T. Vreven, J. A. Montgomery, Jr., J. E. Peralta, F. Ogliaro, M. Bearpark, J. J. Heyd, E. Brothers, K. N. Kudin, V. N. Staroverov, R.

Kobayashi, J. Normand, K. Raghavachari, A. Rendell, J. C. Burant, S. S. Iyengar, J. Tomasi, M. Cossi, N. Rega, J. M. Millam, M. Klene, J. E. Knox, J. B. Cross, V. Bakken, C. Adamo, J. Jaramillo, R. Gomperts, R. E. Stratmann, O. Yazyev, A. J. Austin, R. Cammi, C. Pomelli, J. W. Ochterski, R. L. Martin, K. Morokuma, V. G. Zakrzewski, G. A. Voth, P. Salvador, J. J. Dannenberg, S. Dapprich, A. D. Daniels, Ö. Farkas, J. B. Foresman, J. V.Ortiz, J. Cioslowski, and D. J. Fox, Gaussian, Inc., Wallingford CT, 2009.

[50] H. Chermette, Chemical reactivity indexes in density functional theory, J. Comput. Chem. 20 (1999) 129-154.

[51] R.G. Pearson, Chemical hardness and density functional theory, J. Chem. Sci. 117 (2005) 369-377.

[52] R.G. Parr, L.v. Szentpály, S. Liu, Electrophilicity index, J. Am. Chem. Soc. 121 (1999) 1922-1924.

[53] L. Pauling, The Nature of the Chemical Bond, Cornell university press Ithaca, NY 1960.

[54] S.Wolff, D. Grimwood, J. McKinnon, M. Turner, D. Jayatilaka, M.J.U.o.W.A. Spackman, Perth, Australia, Crystal explorer ver. 3.1, (2013).

[55] J. Dalal, N. Sinha, H. Yadav, B. Kumar, Structural, electrical, ferroelectric and mechanical properties with Hirshfeld surface analysis of novel NLO semiorganic sodium p-nitrophenolate dihydrate piezoelectric single crystal, RSC Adv. 71 (2015) 57735-57748.